PRELIMINARY COMMUNICATION

Use of Florbetapir-PET for Imaging β-Amyloid Pathology

Christopher M. Clark, MD
Julie A. Schneider, MD
Barry J. Bedell, MD, PhD
Thomas G. Beach, MD, PhD
Warren B. Bilker, PhD
Mark A. Mintun, MD
Michael J. Pontecorvo, PhD
Franz Hefti, PhD
Alan P. Carpenter, PhD
Matthew L. Flitter, BA
Michael J. Krautkramer, BS
Hank F. Kung, PhD
R. Edward Coleman, MD
P. Murali Doraiswamy, MD
Adam S. Fleisher, MD, MAS
Marwan N. Sabbagh, MD
Carl H. Sadowsky, MD
Eric M. Reiman, MD
Simone P. Zehntner, PhD
Daniel M. Skovronsky, MD, PhD
for the AV45-A07 Study Group

Context The ability to identify and quantify brain β-amyloid could increase the accuracy of a clinical diagnosis of Alzheimer disease.

Objective To determine if florbetapir F 18 positron emission tomographic (PET) imaging performed during life accurately predicts the presence of β-amyloid in the brain at autopsy.

Design, Setting, and Participants Prospective clinical evaluation conducted February 2009 through March 2010 of florbetapir-PET imaging performed on 35 patients from hospice, long-term care, and community health care facilities near the end of their lives (6 patients to establish the protocol and 29 to validate) compared with immunohistochemistry and silver stain measures of brain β-amyloid after their death used as the reference standard. PET images were also obtained in 74 young individuals (18-50 years) presumed free of brain amyloid to better understand the frequency of a false-positive interpretation of a florbetapir-PET image.

Main Outcome Measures Correlation of florbetapir-PET image interpretation (based on the median of 3 nuclear medicine physicians' ratings) and semiautomated quantification of cortical retention with postmortem β-amyloid burden, neuritic amyloid plaque density, and neuropathological diagnosis of Alzheimer disease in the first 35 participants autopsied (out of 152 individuals enrolled in the PET pathological correlation study).

Results Florbetapir-PET imaging was performed a mean of 99 days (range, 1-377 days) before death for the 29 individuals in the primary analysis cohort. Fifteen of the 29 individuals (51.7%) met pathological criteria for Alzheimer disease. Both visual interpretation of the florbetapir-PET images and mean quantitative estimates of cortical uptake were correlated with presence and quantity of β-amyloid pathology at autopsy as measured by immunohistochemistry (Bonferroni ρ, 0.78 [95% confidence interval, 0.58-0.89]; $P<.001$]) and silver stain neuritic plaque score (Bonferroni ρ, 0.71 [95% confidence interval, 0.47-0.86]; $P<.001$). Florbetapir-PET images and postmortem results rated as positive or negative for β-amyloid agreed in 96% of the 29 individuals in the primary analysis cohort. The florbetapir-PET image was rated as amyloid negative in the 74 younger individuals in the nonautopsy cohort.

Conclusions Florbetapir-PET imaging was correlated with the presence and density of β-amyloid. These data provide evidence that a molecular imaging procedure can identify β-amyloid pathology in the brains of individuals during life. Additional studies are required to understand the appropriate use of florbetapir-PET imaging in the clinical diagnosis of Alzheimer disease and for the prediction of progression to dementia.

JAMA. 2011;305(3):275-283 www.jama.com

BOTH DIAGNOSIS AND TREATMENT of Alzheimer disease (AD) are hampered by the lack of noninvasive biomarkers of the underlying pathology. Between 10% and 20% of patients clinically diagnosed with AD lack AD pathology at autopsy,[1-3] and community physicians may not diagnose AD in 33% of patients with mild signs and symptoms.[4]

See also pp 261 and 304.

Thus, a diagnostic biomarker may help clinicians separate patients who have AD pathology from those who do not.

Author Affiliations are listed at the end of this article.
Corresponding Author: Christopher M. Clark, MD, 3711 Market St, Philadelphia, PA 19104 (clark@avidrp.com).

The latter group is especially important because they require further evaluation to identify the true cause of their cognitive impairment. A pathology-based biomarker also could be useful for the early identification of individuals at risk for developing AD,[5] and to facilitate testing of experimental disease–modifying drugs that target β-amyloid.[6]

The definitive postmortem diagnosis of AD requires the presence of progressive dementia during life and the presence of neuropathological lesions (ie, neuritic plaques composed of β-amyloid aggregates and neurofibrillary tangles formed from hyperphosphorylated tau protein).[7,8] The ^{11}C-labeled Pittsburgh compound B (^{11}C-PiB) was the first positron emission tomographic (PET) ligand to selectively visualize β-amyloid in living patients.[9,10] However, the 20-minute half-life of ^{11}C-PiB limits its use to specialized research centers and highlights the need for ^{18}F-ligands to make β-amyloid PET imaging broadly available.

Several ligands are currently under study, including florbetapir F 18 (^{18}F-AV-45), ^{18}F-flutemetamol (^{18}F-GE067), florbetaben (^{18}F-BAY94-9172), and ^{18}F-FDDNP.[11-14] Of these, florbetapir F 18 (^{18}F-AV-45) is in wide use as a research biomarker in the Alzheimer Disease Neuroimaging Initiative[15] and in several phase 3 clinical trials of experimental AD drugs.

Previous studies with florbetapir F 18 demonstrated high affinity and specificity to β-amyloid and favorable pharmacokinetics.[16,17] It is rapidly cleared from circulation with only 10% remaining 20 minutes after injection. The ligand rapidly enters the brain with clear separation between individuals with and without amyloid seen 20 minutes after injection.[17] In brains presumed to have aggregated β-amyloid, maximum uptake occurs approximately 30 minutes after injection and remains essentially unchanged for the subsequent 60 minutes,[17] providing a wide time window to obtain a 10-minute image. Whole-body radiation dosimetry studies in humans indicated that the organs with the highest exposure are the gallbladder, intestines, liver, and urinary bladder.[16,17] However, the definitive relationship between the florbetapir-PET image and β-amyloid deposition has not been established.

We report the results of the first phase 3 multicenter study, to our knowledge, conducted in individuals at the end of life who consented to both florbetapir-PET imaging and brain donation after death. The goal of the study was to determine the qualitative and quantitative relationship between the florbetapir-PET image and postmortem β-amyloid pathology. PET images also were obtained in younger individuals (age ≤50 years) presumed to be free of brain amyloid to better understand the frequency of a false-positive florbetapir-PET image.

METHODS

From February 2009 through March 2010, the study enrolled 152 individuals approaching the end of life to obtain 35 postmortem evaluations (brain autopsies) from those who received PET imaging 12 months or less prior to death. Individuals were recruited from in-patient and community hospice programs, long-term care facilities, and outpatient community health care facilities. The main inclusion criteria included a physician's assessment that the individual was likely to die within 6 months of study enrollment, absence of any known destructive lesion in the brain (eg, stroke or tumor), and the individual's willingness to have florbetapir-PET imaging followed by a brain autopsy at the time of death. Each participant received a brief physical, neurological, and cognitive evaluation that included assessments of memory, language, and constructional praxis. In the 35 individuals who were autopsied, the major comorbidities were hypertension (66%), cancer (49%), cardiac disease (46%), chronic lung disease (37%), and diabetes (29%). The primary study clinical diagnosis and cause of death (as noted by the study physician) are listed in TABLE 1.

The postmortem evaluations for the first 6 participants were evaluated separately as part of a preplanned interim analysis. The final 29 postmortem evaluations comprised the primary analysis data set.

A second group of 74 young cognitively normal, healthy individuals (aged 18-50 years) were recruited from the community and were evaluated using the same clinical assessment and PET imaging protocol as those in the autopsy cohort to determine (among individuals who presumably had no β-amyloid) the proportion that were categorized correctly by a florbetapir-PET scan as amyloid negative.

For all participants in this study, written informed consent was provided by the individual or by his/her designated decision maker and the study was approved by institutional review boards.

Florbetapir-PET Imaging Acquisition and Interpretation

Participants were imaged at 23 sites using clinical PET and PET/computed tomographic scanners. Each participant underwent a 10-minute PET scan, which began 50 minutes after receiving an intravenous bolus of 370 MBq (10 mCi) florbetapir F 18. Images were acquired with a 128×128 matrix (zoom ×2) and were reconstructed using iterative or row action maximization likelihood algorithms.

Florbetapir-PET images were assessed visually using a semiquantitative score ranging from 0 (no amyloid) to 4 (high levels of cortical amyloid) by 3 board-certified nuclear medicine physicians who were not involved in any other aspects of the study. The only experience these physicians had with florbetapir-PET imaging occurred during a half-day training session. The median rating of the readers served as a primary outcome variable. Readers were blinded to clinical, demographic, and neuropathological information and viewed and rated images under the supervision and at the facility

Table 1. Clinical and Outcome Values for 35 Participants With a Postmortem Evaluation[a]

			Florbetapir-PET Imaging		Autopsy Reference Standard				
								AD Diagnosis	
Clinical Diagnosis Category	Age at Death, y	Cause of Death	SUVr	Median Visual Reading	β-Amyloid IHC	NPS	Braak Stage[18]	CERAD	NIA/Reagan Institute
ODD	87.4	Esophageal cancer	0.81	1	0.02	0	2	No	Low likelihood
AD[b]	82.8	Congestive heart failure	0.87	0	0.15	0	3	No	Low likelihood
MCI	92.2	Congestive heart failure	0.87	0	0.01	0	4	No	Low likelihood
HC	62.5	Respiratory arrest	0.88	0	0.01	0	1	No	Low likelihood
HC	85.9	Respiratory failure	0.88	0	0.01	0	1	No	Low likelihood
HC	84.6	Lung cancer	0.91	1	0.01	0	1	No	Low likelihood
MCI	86.2	Cardiac arrest	0.92	1	0.03	0	3	No	Low likelihood
HC	99.9	Heart failure	0.92	1	0	0	3	No	Low likelihood
HC	62.1	Infection	0.93	0	0.01	0	1	No	Low likelihood
ODD	104.3	End-stage dementia	0.98	0	0.49	1	1	Possible	Low likelihood
HC	70.1	Prostate cancer	1.00	0	0.47	1	1	Possible	Low likelihood
HC	93.2	Acute MI	1.00	1	1.11	0	0	No	No AD
HC	85.7	Hepatic cancer	1.00	1	0	0	3	No	Low likelihood
ODD	73.9	Advanced PD	1.07	0	0.01	0	3	No	Low likelihood
MCI[b]	48.0	Respiratory and renal failure	1.09	1	0	0	1	No	Low likelihood
HC	55.9	Prostate cancer	1.09	0	0.04	0	1	No	Low likelihood
ODD[b]	78.5	Acute respiratory failure	1.17	2	3.63	2	5	Definite	High likelihood
AD	81.5	Respiratory failure	1.20	3	7.01	3	5	Definite	High likelihood
AD	76.3	AD	1.20	3	5.27	2	5	Definite	High likelihood
ODD	88.7	Cardiac and respiratory arrest	1.21	3	1.42	3	5	Definite	High likelihood
AD	88.1	AD	1.23	1	4.85	2	5	Probable	Intermediate likelihood
ODD	67.9	Pick disease and stroke	1.34	4	6.69	2	5	Definite	High likelihood
AD	72.1	AD	1.36	3	5.31	3	6	Definite	High likelihood
AD	91.8	Acute MI	1.37	3	9.11	2	5	Definite	High likelihood
AD	55.5	Cardiac and respiratory arrest	1.38	3	4.67	3	6	Definite	High likelihood
AD[b]	79.8	AD	1.38	4	7.92	2	6	Definite	High likelihood
AD	89.2	Pneumonia	1.39	3	1.48	2	3	Definite	Intermediate likelihood
AD	88.2	Respiratory failure	1.40	3	3.42	2	5	Definite	High likelihood
AD	86.8	AD	1.45	4	3.27	1	4	Probable	Intermediate likelihood
AD[b]	86.5	AD	1.56	3	5.39	3	5	Definite	High likelihood
AD	60.0	Unknown	1.57	4	9.44	3	6	Definite	High likelihood
AD	69.3	Respiratory failure	1.63	4	5.61	2	5	Definite	High likelihood
AD	92.3	AD	1.64	3	1.11	1	4	Probable	Intermediate likelihood
AD[b]	84.6	AD	1.66	4	8.62	3	6	Definite	High likelihood
AD	91.7	AD	1.91	4	5.38	2	4	Probable	Intermediate likelihood

Abbreviations: AD, Alzheimer disease; CERAD, Consortium to Establish a Registry for Alzheimer's Disease; HC, cognitively healthy control; IHC, immunohistochemistry; MCI, mild cognitive impairment; MI, myocardial infarction; NIA/Regan Institute, National Institute on Aging and Reagan Institute Working Group on Diagnostic Criteria for the Neuropathological Assessment of Alzheimer's Disease; NPS, neuritic plaque score; ODD, other dementing disorder; PD, Parkinson disease; PET, positron emission tomographic; SUVr, semiautomated quantitative analysis of the ratio of cortical to cerebellar signal.

[a] Participants are ordered by increasing florbetapir-PET SUVr score.

[b] Indicates participant was in the interim analysis (n=6).

of the imaging core laboratory (ImageMetrix, a division of the American College of Radiology, Philadelphia, Pennsylvania). The initial 6 postmortem evaluations were rated by 4 readers and the median rating of the 4 raters served as the primary outcome variable for these 6 participants.

For the younger control cohort, the PET images were mixed in random order with 40 images from the autopsy cohort that had a median visual read score between 2 and 4 (inclusive). To remove image recognition bias, these images were rated as amyloid positive or negative at ImageMetrix by a different group of 3 external readers. The majority rating was used as the primary outcome variable for this analysis.

A semiautomated quantitative analysis of the ratio of cortical to cerebellar signal (SUVr) also was performed for florbetapir-PET images from all study participants. The images were first normalized to a standard template in the Talairach space and then the SUVrs were calculated for the 6 predefined cortical regions of interest (frontal, temporal, parietal, anterior cingulate, pos-

Figure. Paired Representative Florabetapir-PET Scans and β-Amyloid Antibody 4G8 Immunohistochemistry Photo Micrographs

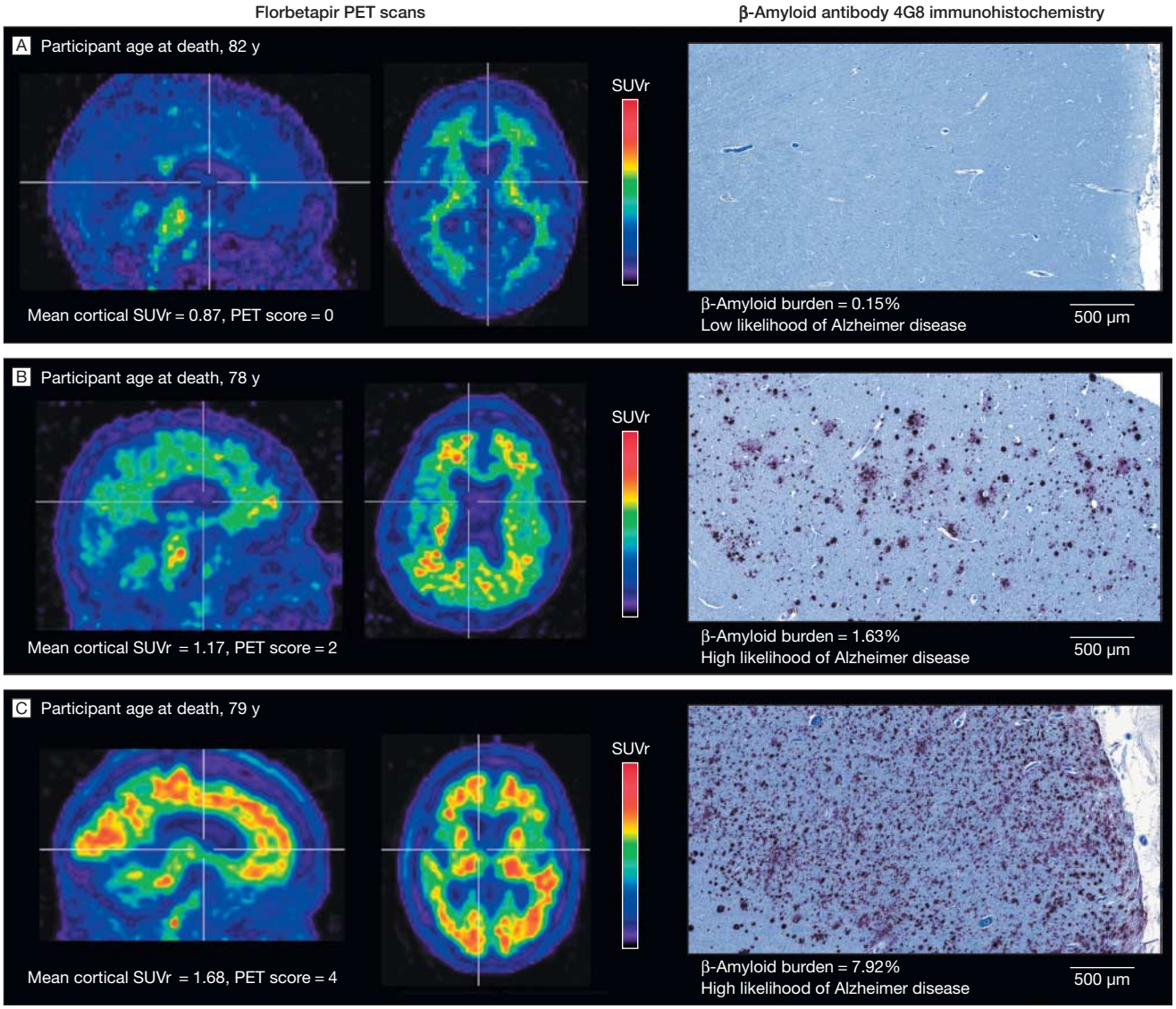

Sagittal and axial views of positron emission tomographic (PET) scans of representative patients. The vertical bars indicate the range of semiautomated quantitative analysis of the ratio of cortical to cerebellar signal (SUVr) scores. The maximum color (red) corresponds to an SUVr of approximately 2.2. The 4G8 immunohistochemistry shows precuneus gray matter with aggregated β-amyloid (red) using a 3-amino-9-ethyl-carbazol chromogen stain and counterstained with acid blue 129 (original magnification ×5).

terior cingulate, and precuneus). The whole cerebellum was used as the reference region.

Neuropathological Evaluation

At the time of death, the brain was removed following standard autopsy procedures and placed in fixative for 2 weeks prior to dissection by an experienced neuropathologist (T.G.B.) at Banner Sun Health Research Institute (Sun City, Arizona). Two or 3 tissue blocks from 7 regions (frontal, temporal, parietal, anterior and posterior cingulate, precuneus, and cerebellum) from both hemispheres were dissected using a standard atlas for guidance. Tissue blocks were processed, embedded in paraffin, and two 6-µm thick tissue sections from each block, separated by approximately 500 µm, were cut and mounted on slides.

Two independent methods were used to identify and quantify β-amyloid aggregation. The β-amyloid antibody 4G8 (1:2000 dilution; Covance, Emeryville, California) was used to quantify β-amyloid aggregation in tissue sections using an automated immunostainer and following established immunohistochemistry methods. Visualization was accomplished using ultravision polymer-horseradish peroxidase amplification (Laboratory Vision, Freemont, California) and detected with 3-amino-9-ethylcarbazole chromogen, which was counterstained with acid blue 129. The stained slides were digitized using a high-resolution, automated slide scanner Zeiss MIRAX (Carl Zeiss Canada Ltd, Toronto, Ontario, Canada).

Image quantification was performed using the Permits image processing and analysis software (Biospective Inc, Montreal, Quebec, Canada). This automated quantification method segments chromogen-positive pixels to generate a parametric map of β-amyloid positivity. The β-amyloid burden (percentage of gray matter containing β-amyloid aggregates) was calculated for each tissue section. The value for each anatomical region was based on the mean obtained using values from all slides from that region (FIGURE).

β-Amyloid neuritic plaque density was determined using a Bielschowsky silver stain applied to 6-µm thick sections from each cortical region of interest and the cerebellum (Rush University Medical Center, Chicago, Illinois). Plaque density was scored on 2 sections from each anatomical region by 2 independent experienced neuropathology raters and was reviewed by a senior neuropathologist (J.A.S.). All of the raters were blinded to the participant's demographic, clinical, and imaging results. The mean density for both neuritic and diffuse plaques was summarized by anatomical region using a 4-point semiquantitative scale (0=none, 1=sparse, 2=moderate, 3=severe).

In addition, a neuropathological diagnosis was made using standardized criteria as described by Braak and Braak,[18] the Consortium to Establish a Registry for Alzheimer's Disease (CERAD)[19] (modified to exclude age and clinical information), and the National Institute on Aging (NIA) and Reagan Institute Working Group on Diagnostic Criteria for the Neuropathological Assessment of Alzheimer's Disease (NIA/Reagan Institute criteria).[8] The pathological diagnosis of AD was independently confirmed by a second neuropathologist (T.G.B.). There was complete agreement by the neuropathologists for all participants with a diagnosis of AD. The final neuropathological diagnosis for all 35 participants in the autopsy cohort is provided in the eTable at http://www.jama.com.

Table 2. Key Correlations for the Primary Analysis Cohort (n = 29)[a]

Cortex Region	Florbetapir-PET Measure	Pathology Reference Standard	Bonferroni ρ (95% CI)
Whole brain	Visual	β-Amyloid area	0.78 (0.58-0.89)
Whole brain	SUVr	β-Amyloid area	0.75 (0.53-0.88)
Whole brain	Visual	NPS	0.71 (0.47-0.86)
Whole brain	SUVr	NPS	0.74 (0.51-0.87)
Whole brain	SUVr vs visual	NA	0.82 (0.64-0.91)
Whole brain	NA	β-Amyloid area vs NPS	0.88 (0.76-0.94)
Precuneus	Visual	β-Amyloid area	0.75 (0.54-0.88)
Parietal	Visual	β-Amyloid area	0.77 (0.56-0.89)
Frontal	Visual	β-Amyloid area	0.69 (0.44-0.85)
Temporal	Visual	β-Amyloid area	0.68 (0.42-0.84)
Posterior cingulate	Visual	β-Amyloid area	0.70 (0.44-0.85)
Anterior cingulate	Visual	β-Amyloid area	0.74 (0.51-0.87)

Abbreviations: CI, confidence interval; NA, data not available; NPS, neuritic plaque score; PET, positron emission tomographic; SUVr, semiautomated quantitative analysis of the ratio of cortical to cerebellar PET signal.
[a]Correlations were assessed between key florbetapir-PET imaging measures and key pathological measures using the Spearman rank correlation coefficient.

Statistical Analysis

Correlations of Florbetapir-PET Signal With Postmortem Histopathology. The correlations between the florbetapir-PET signal (measured by visual score or SUVr) and cortical β-amyloid pathology (measured by immunohistochemistry or by silver stain) were evaluated using the Spearman rank correlation coefficient. The primary analysis tested the correlation between the semiquantitative visual rating of global cortical ligand retention on florbetapir-PET and the mean cortical β-amyloid in the corresponding tissue as determined by quantitative immunohistochemistry. Adjustment was made for multiple comparisons for the 13 correlation tests using the Bonferroni method. The experiment-wise type I error rate was 5%. In TABLE 2, all of the *P* values were less than .001 for each row of data; the *P* values were multi-

plied by 13 to adjust for multiple comparisons. Sample size calculations were performed using a correlation of 0.55, giving the study 90% power to detect a significant correlation in the primary analysis with 29 participants to be evaluated by autopsy. Except where indicated, correlations are based on data from the 29 participants in the primary analysis cohort. There were no significant differences when the analysis was repeated using all 35 autopsied participants.

Analysis in the Young Healthy Cohort. A second co-primary hypothesis was that 90% or greater of the young healthy participants negative for the apolipoprotein E ε4 (*ApoE ε4*) allele would have a florbetapir-PET image that was read as β-amyloid negative. Analysis included calculation of the upper and lower 95% confidence intervals (CIs) for the percentage read as negative. Sample size calculations indicated that 40 participants would be sufficient to ensure that the lower 95% CI would be 80% or greater if the hypothesis was true. STATA version 11.1 (StataCorp, College Station, Texas) was used to perform all statistical analyses.

RESULTS

Of the 152 participants in the study, 2 were withdrawn by the site investigator for excessive movement artifact. Images were not acquired for 3 participants because of a PET camera failure, leaving 147 participants with valid images. Two participants died without autopsy (consent withdrawn by the family at the time of death). Table 1 lists the study diagnostic category, age at death, and clinician-noted cause of death for each of the 35 participants who were autopsied. The first 6 participants were used in an interim analysis and the next 29 were used in the primary analysis.

In the primary analysis cohort (n=29), the mean interval from florbetapir-PET imaging to death was 99 days (range, 1-377 days). Based on the assessment of the enrolling physician, the cognitive status of individuals in the autopsy cohort varied from having normal cognition to severe dementia at the time of imaging (TABLE 3). Among the 29 individuals in the primary analysis cohort, 31% were not considered to be cognitively impaired by the enrolling physician, 7% were considered mildly impaired but without dementia, 45% had a clinical diagnosis of AD, and 17% had a clinical diagnosis of a non-AD dementia.

Of the 74 young healthy participants, 47 had genotyping that was negative for the *ApoE ε4* allele. Characteristics of these participants are summarized in TABLE 4. All 74, including those carrying the *ApoE ε4* allele, had a florbetapir-PET image that was rated as amyloid negative. There was good agreement among the nuclear medicine physicians' visual ratings of the florbetapir-PET images. Pairwise agreement ranged from 91% (κ=0.68) to 99% (κ=0.98).

Table 1 summarizes the imaging and autopsy results from all 35 participants who were autopsied (ie, the 29 participants in the primary analysis autopsy cohort plus the 6 participants from the interim analysis portion of the study). As shown in Table 2, there was good correlation between the whole-brain florbetapir-PET visual image scores and the postmortem amyloid pathology as measured by immunohistochemistry (Bonferroni ρ, 0.78 [95% CI, 0.58-0.89]; $P<.001$) and silver stain neuritic plaque score (Bonferroni ρ, 0.71 [95% CI, 0.47-0.86]; $P<.001$). Similarly, there was good correlation between the whole brain SUVr and amyloid burden as measured by immuno-

Table 3. Demographic and Clinical Description of Study Participants

		Postmortem Examination	
	Received PET (N = 152)	Analysis Cohort (n = 29)	All Participants (n = 35)
Age, mean (range), y	78.1 (38-103)	80.0 (55-103)	79.3 (47-103)
Male sex, No. (%)	71 (46.7)	15 (51.7)	18 (51.4)
Education, mean (SD), y	13.1 (2.68)	13.4 (2.50)	13.1 (2.56)
Diagnosis, No. (%)			
Alzheimer disease	56 (37)	13 (44.8)	17 (48.6)
Mild cognitive impairment	25 (16)	3 (6.8)	3 (8.6)
Other dementing disorder	21 (14)	5 (17.2)	6 (17.1)
Cognitively normal	50 (33)	9 (31)	9 (25.7)
Mini-Mental State Examination score, mean (SD)	(n = 115) 21.2 (9.3)	(n = 21) 19.9 (10.0)	(n = 26) 18.1 (10.2)
Weschler Memory (delayed) scale score, mean (SD)	(n = 107) 5.1 (4.8)	(n = 19) 3.9 (4.5)	(n = 22) 3.8 (4.3)
Interval, mean (SD)			
PET scan to death, d		99.4 (73.4)	89.4 (73.5)
Death to autopsy, h		11.7 (9.0)	11.2 (8.6)

Abbreviation: PET, positron emission tomography.

Table 4. Young Cognitively Normal Participants

	Total (n = 74)	Without *ApoE ε4* Allele (n = 47)
Age, mean (range), y	26.7 (18-50)	26.3 (18-50)
Male sex, No. (%)	48 (64.9)	32 (68.1)
Education, mean (SD), y	14.4 (2.24)	14.4 (2.41)
Score, mean (SD)		
Mini-Mental State Examination	29.7 (0.57)	29.8 (0.40)
Weschler Memory (delayed) scale	15.4 (3.46)	15.5 (2.84)

Abbreviation: *ApoE ε4*, apolipoprotein E ε4.

histochemistry (Bonferroni ρ, 0.75 [95% CI, 0.53-0.88]; $P<.001$) and by neuritic plaque score (Bonferroni ρ, 0.74 [95% CI, 0.51-0.87]; $P<.001$). For each of the 6 cortical regions, there were good correlations between florbetapir-PET signal and postmortem measurement of amyloid in the corresponding region (range of Bonferroni ρ: 0.68 [95% CI, 0.42-0.84] to 0.77 [95% CI, 0.56-0.89]). Inclusion of the 6 autopsied participants from the interim analysis did not significantly alter these results (*P* values were all smaller).

There were significant correlations observed between the 2 measures of amyloid on florbetapir-PET (SUVr vs semiquantitative visual score: Bonferroni ρ, 0.82 [95% CI, 0.64-0.87]; $P<.001$) and the 2 measures of amyloid aggregation at autopsy (immunohistochemistry vs silver stain: Bonferroni ρ, 0.88 [95% CI, 0.76-0.94]; $P<.001$). The strength of the intermethod correlations (eg, PET visual read to immunohistochemistry) were similar to that for the intramethod correlations (eg, PET visual read to PET SUVr, pathology immunohistochemistry to pathology plaque score).

Fifteen participants in the primary analysis autopsy cohort met pathological criteria for AD (CERAD: probable or definite AD; NIA/Reagan Institute criteria: intermediate to high likelihood of AD). Of these 15 participants, 14 had florbetapir-PET scans that were interpreted as visually positive (median read ≥2), giving a sensitivity of 93% (95% CI, 68%-100%).

Fourteen participants in the autopsy cohort had low levels of β-amyloid aggregation on the postmortem examination and did not meet CERAD or NIA/Reagan Institute pathological criteria for AD. All 14 had florbetapir-PET scans that read as negative, yielding a specificity of 100% (95% CI, 76.8%-100%).

In total, the blinded read results for the florbetapir-PET images agreed with the final autopsy with respect to the presence or absence of neuropathological criteria of AD in 28 of 29 cases. The neuropathological diagnosis in the participants who did not meet pathological criteria for AD included dementia with Lewy bodies, hippocampal sclerosis, Parkinson disease, subcortical microscopic infarcts, mesial temporal lobe neurofibrillary tangles, neurofibrillary tangles with argyrophilic grains and glial tauopathy, and no neuropathology (eTable at http://www.jama.com).

On an exploratory basis, the clinical diagnosis was compared with the final autopsy diagnosis. Of the 15 participants in the autopsy cohort who had dementia diagnoses in life (AD or other dementias), the clinical diagnosis did not match the final autopsy diagnosis in 3 (20%). Of these 3, one was diagnosed with probable AD in life (but was negative for AD at autopsy) and 2 were clinically diagnosed with other dementing disorders (1 each with Parkinson disease dementia and Lewy body dementia, but both received a final autopsy diagnosis of AD) (eTable). Florbetapir-PET imaging correctly predicted the presence or absence of significant β-amyloid pathology in all 3 participants.

COMMENT

Before florbetapir-PET measures of β-amyloid can be accepted in clinical practice, the degree to which the imaging ligand accurately identifies pathology in living patients must be clearly demonstrated. Based on autopsy reports and imaging and nonimaging data, it is increasingly accepted that the pathology of AD may begin years prior to symptomatic cognitive decline.[20-29] A valid imaging-to-autopsy correlation study can only be accomplished by minimizing the interval between florbetapir-PET imaging and measuring the degree of β-amyloid pathology. To accomplish this goal, we recruited individuals approaching the end of life to demonstrate that findings on florbetapir-PET images are consistent with the presence and density of cortical β-amyloid aggregates found at autopsy.

The ability of this molecular imaging ligand to identify a key pathological signature of AD was demonstrated using both an objective automated immunohistochemistry measurement to quantify the β-amyloid burden and a traditional silver stain to identify and quantify the density of neuritic amyloid plaques. These measures of AD-associated pathology correlated well with both the visual assessment of the florbetapir-PET scan and the mean cortical SUVr (an automated quantitative measure of regional ligand retention in 6 predefined cortical areas). Ours are the first prospective, multicenter results that demonstrate it is possible to both directly identify and quantify the presence of β-amyloid aggregates using a molecular imaging procedure. This technique will allow future studies to identify the presence of β-amyloid in the brains of individuals when the symptoms are quite mild, and many years before their death.

The development of standardized clinical criteria for the diagnosis of AD[7] in 1984 provided guidelines that could be used to increase the validity of the diagnosis while allowing for a degree of uncertainty. The magnitude of this uncertainty is reflected in the failure to find postmortem evidence of AD pathology in up to 20% of patients diagnosed with AD during life. A proposal to include pathologically-linked biomarkers of AD in the clinical diagnostic criteria[30] has the potential to improve diagnostic accuracy, especially at the earliest symptomatic stage.

Our study suggests that a florbetapir-PET image provides an accurate and reliable assessment of amyloid burden. However, while amyloid pathology is a sine qua non for an AD diagnosis, clinically impaired function may depend, in part, on the ability of the individual's brain to tolerate aggregated amyloid. Genetic risk factors, lifestyle choices, environmental factors, and neuropathological comorbidities may alter the threshold for the onset of cognitive impairment associated with β-amyloid aggregation.[31,32]

There is now a growing body of evidence that the presence of β-amyloid aggregates in individuals prior to de-

veloping AD is a significant and independent risk factor for cognitive impairment and eventual development of AD.[26,33,34] Therefore, brain florbetapir-PET imaging of β-amyloid aggregates has the potential to improve selection and monitoring of patients considered candidates for studies of disease-modifying AD treatments.

Our study has several limitations, including the relatively small sample size of the autopsy cohort (n=35) and the use of a young, cognitively healthy nonautopsy cohort to determine the likelihood that a florbetapir-PET image would falsely suggest the presence of aggregated amyloid. The readings were performed by 3 trained nuclear medicine physicians and the median of the 3 results was used in the analysis, which is a process not likely to be replicated in clinical settings. Additionally, the individuals who participated in this study do not represent those who would typically be undergoing an evaluation for new-onset cognitive impairment, but rather were selected for their unique ability to provide information about the ability of florbetapir-PET imaging to accurately identify and quantify β-amyloid with the shortest interval between imaging and definitive pathological evaluation possible. Furthermore, standardized criteria for AD and mild cognitive impairment were not used.

CONCLUSIONS

Florbetapir-PET imaging performed during life in this study correlated with the presence and density of β-amyloid at autopsy. This prospective imaging to autopsy study provides evidence that a molecular imaging procedure can identify β-amyloid pathology in the brains of individuals during life. Understanding the appropriate use of florbetapir-PET imaging in the clinical diagnosis of AD or in the prediction of progression to dementia will require additional studies.

Author Affiliations: Avid Radiopharmaceuticals, Philadelphia, Pennsylvania (Drs Clark, Mintun, Pontecorvo, Hefti, Carpenter, and Skovronsky and Messrs Flitter and Krautkramer); School of Medicine, University of Pennsylvania, Philadelphia (Drs Clark, Bilker, Kung, and Skovronsky); Rush University Medical Center, Chicago, Illinois (Dr Schneider); Biospective Inc, Montreal, Quebec, Canada (Drs Bedell and Zehntner); Montreal Neurological Institute, McGill University, Montreal, Quebec, Canada (Dr Bedell); Banner Sun Health Research Institute, Phoenix, Arizona (Drs Beach and Sabbagh); School of Medicine, Washington University, St Louis, Missouri (Dr Mintun); Duke University Medical Center, Durham, North Carolina (Drs Coleman and Doraiswamy); Banner Alzheimer's Institute, Phoenix, Arizona (Drs Fleisher and Reiman); Department of Neurosciences, University of California, San Diego (Dr Fleisher); Department of Medicine, Division of Neurology, Nova SE University, Ft Lauderdale, Florida (Dr Sadowsky); Arizona Alzheimer's Consortium, Phoenix (Dr Reiman); and Department of Psychiatry, College of Medicine, University of Arizona, Phoenix (Dr Reiman).

Author Contributions: Dr Schneider had full access to all of the data in the study and takes responsibility for the integrity of the data and the accuracy of the data analysis.

Study concept and design: Clark, Bedell, Beach, Mintun, Pontecorvo, Hefti, Carpenter, Flitter, Kung, Sadowsky, Reiman, Skovronsky.

Acquisition of data: Clark, Schneider, Bedell, Beach, Pontecorvo, Flitter, Coleman, Doraiswamy, Fleisher, Sabbagh, Sadowsky, Reiman, Zehntner, Skovronsky.

Analysis and interpretation of data: Clark, Bedell, Bilker, Mintun, Pontecorvo, Hefti, Flitter, Krautkramer, Fleisher, Sadowsky, Skovronsky.

Drafting of the manuscript: Clark, Bedell, Beach, Pontecorvo, Hefti, Flitter, Kung, Fleisher, Sadowsky, Zehntner, Skovronsky.

Critical revision of the manuscript for important intellectual content: Clark, Schneider, Bedell, Beach, Bilker, Mintun, Pontecorvo, Hefti, Carpenter, Krautkramer, Coleman, Doraiswamy, Fleisher, Sabbagh, Sadowsky, Reiman, Skovronsky.

Statistical analysis: Clark, Bedell, Bilker, Skovronsky.

Obtained funding: Kung, Coleman, Skovronsky.

Administrative, technical, or material support: Schneider, Bedell, Beach, Hefti, Carpenter, Flitter, Krautkramer, Doraiswamy, Sadowsky, Skovronsky.

Study supervision: Clark, Beach, Pontecorvo, Flitter, Krautkramer, Kung, Sadowsky, Reiman, Skovronsky.

Conflict of Interest Disclosures: All authors have completed and submitted the ICMJE Form for Disclosure of Potential Conflicts of Interest. Drs Clark, Mintun, Pontecorvo, Hefti, Carpenter, and Skovronsky and Messrs Flitter and Krautkramer reported owning Avid stock and/or stock options and being employed by Avid Radiopharmaceuticals Inc. Dr Schneider reported being a consultant for Avid Radiopharmaceuticals and receiving compensation for services. Drs Bedell and Zehntner reported receiving compensation and shares from Biospective Inc. Dr Beach reported receiving funding related to the topic of this article from the National Institute on Aging (grant P30 AG19610), the Arizona Department of Health Services (contract 211002 awarded to the Arizona Alzheimer's Research Center), the Arizona Biomedical Research Commission (contracts 4001, 0011, 05-901 and 1001), Avid Radiopharmaceuticals, Bayer Healthcare Inc, and GE Healthcare. Dr Bilker reported working as consultant for Avid Radiopharmaceuticals on issues related to this study. Dr Kung reported receiving financial support from National Institutes of Health grant AG-0222559; serving on the Avid Scientific Advisory board; participating in the formation of Avid; and being an Avid stockholder. Dr Coleman reported being on the medical advisory board for General Electric Healthcare from 2003-2008; being a consultant for General Electric Healthcare from 2003-2008; receiving a research grant from General Electric Healthcare in 2010; receiving funding for a clinical trial from Molecular Insights Pharmaceuticals in 2010; serving on a medical advisory board for Molecular Insights Pharmaceuticals from 2004-2009; and receiving a grant from Avid to support his participation in this study. Dr Doraiswamy reported receiving research grants (awarded to Duke University); currently or previously serving as an advisor to Forest, Bristol-Myers Squibb, Avid Radiopharmaceuticals, Lundbeck, Medivation, Pfizer, Elan, Eli Lilly, Bayer, Neuroptix, Neuronetrix, Sonexa, Accera, TauRx, Myriad, National Institute on Aging, AstraZeneca, Labopharm, Clarimedix, National Institute of Mental Health, National Institute of Neurological Disorders and Stroke, Alzheimer's Association, Alzheimer's Foundation, Rutgers University, and the University of California; owning stock in Sonexa; and receiving a grant from Avid (awarded to Duke University) for his participation in this study. Dr Fleisher reported receiving research contracts from Avid Radiopharmaceuticals to the Banner Alzheimer's Institute, from which he receives no personal compensation; being a consultant on a scientific advisory board for Eli Lilly; serving on an advisory board for Elan Pharmaceuticals; and having a pending investigator-initiated grant from Avid Radiopharmaceuticals. Dr Sabbagh reported working as a consultant for Eisai, Pfizer, Amerisciences, Takeda, and GlaxoSmithKline; receiving royalties from Wiley, FT Pearson Press, and Amerisciences; and having grants and contracts with Eli Lilly, Baxter, Bayer, General Electric Healthcare, Bristol-Myers Squibb, Eisai, Janssen, Wyeth/Elan, Avid, and Medivation. Dr Sadowsky reported being on the speaker's bureau and receiving honoraria from Novartis, Forrest, Accera, and Pamlab; and serving on the advisory board for Novartis. Dr Reiman reported serving as a scientific advisor to Amnestix/Sygnis, AstraZeneca, Elan, Eli Lilly, GlaxoSmithKline, Intellect, Siemens, Bayer, Takeda, and Eisai; having research contracts with the National Institute on Aging, Arizona Department of Health Services, AstraZeneca, Avid Radiopharmaceuticals, and Kronos Life Sciences; receiving research grants from the National Institute on Aging, National Institute for Mental Health, the Anonymous Foundation, Nomis Foundation, Banner Alzheimer's Foundation, and the State of Arizona; holding patents for imaging strategy for the screening of AD treatments in laboratory animals (active), biomarker strategy for the evaluation of presymptomatic AD treatments (pending, through Banner Health), statistical strategy for the analysis of complementary complex data sets (pending, through Banner Health), and *GAB2* testing in clinical assessment of AD (pending, through Translational Genomics Research Institute); and serving as the executive director for the Banner Alzheimer's Institute and the director of the Arizona Alzheimer's Consortium.

Funding/Support: This study was funded by Avid Radiopharmaceuticals Inc and by grants R01AG031581, P30AG19610, and AG-0222559 from the National Institute on Aging, contract 211002 from the Arizona Department of Health Services, contracts 4001, 0011, 1001, and 05-901 from the Arizona Biomedical Research Commission, and funding from the Michael J. Fox Foundation for Parkinson's Research.

Role of the Sponsor: Avid Radiopharmaceuticals had a role in the design and conduct of the study, Documents Solutions Group (Malvern, Pennsylvania) and Pharmaceutical Product Development Inc (Wilmington, North Carolina) had a role in collection and management of the data, but none had a role in the analysis and interpretation of the data, or in the preparation of the manuscript.

Independent Statistical Analysis: The statistical analysis of the data was conducted independently from the sponsor by coauthor Warren B. Bilker, PhD (Department of Biostatistics and Epidemiology, School of Medicine, University of Pennsylvania, Philadelphia). Dr Bilker received the entire raw data set and ran the analysis and was compensated for this work.

Previous Presentation: Presented in part at the 10th International Conference on Alzheimer's Disease; July 11-16, 2010; Honolulu, Hawaii.

Online-Only Material: The eTable is available at http://www.jama.com.
Additional Contributions: We acknowledge the altruism of the participants and their families as well as the contributions of the AV45-A07 research and support staffs at each of the participating sites, all of whom contributed to this study.

REFERENCES

1. Jobst KA, Barnetson LP, Shepstone BJ. Accurate prediction of histologically confirmed Alzheimer's disease and the differential diagnosis of dementia. *Int Psychogeriatr*. 1998;10(3):271-302.
2. Mayeux R, Saunders AM, Shea S, et al. Utility of the apolipoprotein E genotype in the diagnosis of Alzheimer's disease. *N Engl J Med*. 1998;338(8):506-511.
3. Ranginwala NA, Hynan LS, Weiner MF, White CL III. Clinical criteria for the diagnosis of Alzheimer disease. *Am J Geriatr Psychiatry*. 2008;16(5):384-388.
4. Löppönen M, Räihä I, Isoaho R. Diagnosing cognitive impairment and dementia in primary health care. *Age Ageing*. 2003;32(6):606-612.
5. Thal LJ, Kantarci K, Reiman EM, et al. The role of biomarkers in clinical trials for Alzheimer disease. *Alzheimer Dis Assoc Disord*. 2006;20(1):6-15.
6. Mathis CA, Lopresti BJ, Klunk WE. Impact of amyloid imaging on drug development in Alzheimer's disease. *Nucl Med Biol*. 2007;34(7):809-822.
7. McKhann G, Drachman D, Folstein M, et al. Clinical diagnosis of Alzheimer's disease. *Neurology*. 1984;34(7):939-944.
8. The National Institute on Aging; Reagan Institute Working Group on Diagnostic Criteria for the Neuropathological Assessment of Alzheimer's Disease. Consensus recommendations for the postmortem diagnosis of Alzheimer's disease. *Neurobiol Aging*. 1997;18(4 suppl):S1-S2.
9. Klunk WE, Wang Y, Huang GF, et al. Uncharged thioflavin-T derivatives bind to amyloid-beta protein with high affinity and readily enter the brain. *Life Sci*. 2001;69(13):1471-1484.
10. Klunk WE, Engler H, Nordberg A, et al. Imaging brain amyloid in Alzheimer's disease with Pittsburgh Compound-B. *Ann Neurol*. 2004;55(3):306-319.
11. Koole M, Lewis DM, Buckley C, et al. Whole-body biodistribution and radiation dosimetry of 18F-GE067. *J Nucl Med*. 2009;50(5):818-822.
12. Kung HF, Choi SR, Qu W, et al. 18F Stilbenes and styrylpyridines for PET imaging of a beta plaques in Alzheimer's disease. *J Med Chem*. 2010;53(3):933-941.
13. Rowe CC, Ackerman U, Browne W, et al. Imaging of amyloid beta in Alzheimer's disease with 18F-BAY94-9172, a novel PET tracer. *Lancet Neurol*. 2008;7(2):129-135.
14. Small GW, Kepe V, Ercoli LM, et al. PET of brain amyloid and tau in mild cognitive impairment. *N Engl J Med*. 2006;355(25):2652-2663.
15. Jagust WJ, Bandy D, Chen K, et al. The Alzheimer's Disease Neuroimaging Initiative positron emission tomography core. *Alzheimers Dement*. 2010;6(3):221-229.
16. Lin KJ, Hsu WC, Hsiao IT, et al. Whole-body biodistribution and brain PET imaging with [18F]AV-45, a novel amyloid imaging agent. *Nucl Med Biol*. 2010;37(4):497-508.
17. Wong DF, Rosenberg PB, Zhou Y, et al. In vivo imaging of amyloid deposition in Alzheimer disease using the radioligand 18F-AV-45 (florbetapir [corrected] F 18). *J Nucl Med*. 2010;51(6):913-920.
18. Braak H, Braak E. Evolution of the neuropathology of Alzheimer's disease. *Acta Neurol Scand Suppl*. 1996;165:3-12.
19. Mirra SS, Heyman A, McKeel D, et al. The Consortium to Establish a Registry for Alzheimer's Disease (CERAD). *Neurology*. 1991;41(4):479-486.
20. Hulette CM, Welsh-Bohmer KA, Murray MG, et al. Neuropathological and neuropsychological changes in "normal" aging. *J Neuropathol Exp Neurol*. 1998;57(12):1168-1174.
21. Jack CR Jr, Knopman DS, Jagust WJ, et al. Hypothetical model of dynamic biomarkers of the Alzheimer's pathological cascade. *Lancet Neurol*. 2010;9(1):119-128.
22. Morris JC, Price AL. Pathologic correlates of nondemented aging, mild cognitive impairment, and early-stage Alzheimer's disease. *J Mol Neurosci*. 2001;17(2):101-118.
23. Price JL, Morris JC. Tangles and plaques in nondemented aging and "preclinical" Alzheimer's disease. *Ann Neurol*. 1999;45(3):358-368.
24. Rowe CC, Ellis KA, Rimajova M, et al. Amyloid imaging results from the Australian Imaging, Biomarkers and Lifestyle (AIBL) study of aging. *Neurobiol Aging*. 2010;31(8):1275-1283.
25. Bourgeat P, Chételat G, Villemagne VL, et al. Beta-amyloid burden in the temporal neocortex is related to hippocampal atrophy in elderly subjects without dementia. *Neurology*. 2010;74(2):121-127.
26. Morris JC, Roe CM, Grant EA, et al. Pittsburgh compound B imaging and prediction of progression from cognitive normality to symptomatic Alzheimer disease. *Arch Neurol*. 2009;66(12):1469-1475.
27. Villemagne VL, Pike KE, Darby D, et al. A beta deposits in older non-demented individuals with cognitive decline are indicative of preclinical Alzheimer's disease. *Neuropsychologia*. 2008;46(6):1688-1697.
28. Resnick SM, Sojkova J, Zhou Y, et al. Longitudinal cognitive decline is associated with fibrillar amyloid-beta measured by [11C]PiB. *Neurology*. 2010;74(10):807-815.
29. Fagan AM, Roe CM, Xiong C, et al. Cerebrospinal fluid tau/beta-amyloid(42) ratio as a prediction of cognitive decline in nondemented older adults. *Arch Neurol*. 2007;64(3):343-349.
30. Dubois B, Feldman HH, Jacova C, et al. Research criteria for the diagnosis of Alzheimer's disease. *Lancet Neurol*. 2007;6(8):734-746.
31. Bennett DA, Schneider JA, Arvanitakis Z, et al. Neuropathology of older persons without cognitive impairment from two community-based studies. *Neurology*. 2006;66(12):1837-1844.
32. Schneider JA, Arvanitakis Z, Leurgans SE, Bennett DA. The neuropathology of probable Alzheimer disease and mild cognitive impairment. *Ann Neurol*. 2009;66(2):200-208.
33. Storandt M, Mintun MA, Head D, Morris JC. Cognitive decline and brain volume loss as signatures of cerebral amyloid-beta peptide deposition identified with Pittsburgh compound B. *Arch Neurol*. 2009;66(12):1476-1481.
34. Fagan AM, Mintun MA, Mach RH, et al. Inverse relation between in vivo amyloid imaging load and cerebrospinal fluid A beta 42 in humans. *Ann Neurol*. 2006;59(3):512-519.